FACTA UNIVERSITATIS
Series: **Physics, Chemistry and Technology** Vol. 4, N^o 2, 2006, pp 331 -339

Phenomenology of New Vector Resonances at Future e^+e^- Colliders

M. Gintner[1], **I. Melo**[2], **B. Trpišová**[3]

[123] Department of Physics, University of Žilina, 01026 Žilina, Slovak Republic

Abstract. *We study a possible production of new vector resonances at future* e^+e^- *colliders. The new resonances are associated with new strong physics that could be responsible for electroweak symmetry breaking. Since the new resonances exhibit enhanced couplings to the W and Z bosons as well as to the top quark we concentrate on two processes:* $e^+e^- \to t\bar{t}$ *, and* $e^+e^- \to \nu_e\bar{\nu}_e t\bar{t}$ *in which the vector resonance is produced in the subprocess* $W_LW_L \to t\bar{t}$*. We calculate the cross sections of these processes as well as of the relevant backgrounds.*

Key words: *strong electroweak symmetry breaking, vector resonance, top quark, W and Z bosons,* W_LW_L*-scattering,* ρ*-resonance model, no-resonance model, statistical significance*

1. INTRODUCTION

The mechanism of electroweak symmetry breaking (ESB), responsible for the masses of gauge bosons, and perhaps fermions, remains an unsolved problem in elementary particle physics. Global ESB gives rise to the massless Goldstone bosons. After introducing the Higgs mechanism, the local electroweak symmetry is spontaneously broken and the Goldstone bosons become longitudinal components of originally massless $W^\pm$ and Z bosons. If the coming experiments, LC and LHC, exclude the existence of the the Standard Model (SM) Higgs boson the alternative mechanism behind ESB could be strongly interacting new physics (strong electroweak symmetry breaking – SESB), originally introduced as a scaled-up analogy of the QCD.

In the absence of the SM Higgs boson scattering amplitudes of such processes as $WW \to WW$ violate a tree-level S-matrix unitarity at a TeV scale. In models of SESB new composite resonances are expected to appear to unitarize these scattering amplitudes and we expect their masses to be around the TeV scale as well.

Received: 15 October 2005

A number of studies have concentrated on the production and signatures of the resonances in $W_L W_L \to W_L W_L$ scattering at future lepton and hadron colliders [1]. In our paper we study the $W_L W_L \to t\bar{t}$ scattering as a subprocess of $e^+e^- \to \nu_e\bar{\nu}_e t\bar{t}$ (Fig. 1) and the direct production of the vector resonance in $e^+e^- \to t\bar{t}$. The main appeal of studying these processes lies in the possibility to test the role of the top quark in ESB [1, 2]. This is due to the fact that the scales of the masses of the t-quark and the W and Z bosons are very close. Thus a question arises whether the mechanism of generation of their masses is the same, *i.e.* the new strong interactions responsible for SESB or whether there are some additional new strong interactions introduced just to explain the top mass.

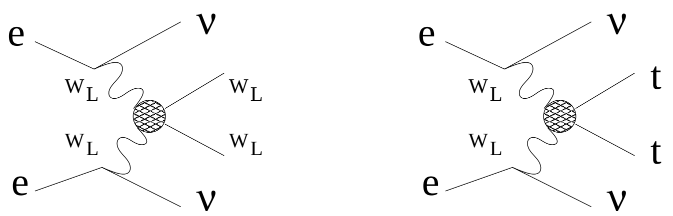

Figure 1: Schematical view of the processes $e^+e^- \to \nu_e\bar{\nu}_e W_L W_L$ and $e^+e^- \to \nu_e\bar{\nu}_e t\bar{t}$ the subprocess of which is the $W_L W_L$ scattering.

To unitarize the VV scattering amplitudes ($V = W, Z$) the simplest solution would be to introduce either a scalar isoscalar $\mathrm{SU}(2)_V$ resonance S, or a vector isovector resonance ρ. While we have studied the S-resonance case elsewhere [3], in this paper we focus on the ρ-resonance which is introduced as a new gauge boson triplet following the BESS (Breaking Electroweak Symmetry Strongly) model [4] approach.

2. ρ-RESONANCE MODEL

In the original version of the BESS model [4] it is assumed that all fermion generations of the same chirality couple to the vector resonance with the same strength. This leads to stringent limits on the resonance-to-fermion couplings from the existing measurements of the SM parameters. In our modification [3] only the third generation of quarks couples directly to the vector resonance of which the right-handed bottom quark does not interact with the vector resonance at all. In this way we avoid the very stringent limits on the ρ-to-fermion couplings that come from the measurements of the $Zb\bar{b}$ vertex.

Our model is based on the non-linear sigma model which is $SU(2)_L \times U(1)_Y$ gauged. The corresponding effective Lagrangian is discussed in detail in our previous paper [3]. Here we show only the fermion part of the model which describes the interaction of the ρ-resonance vector field $\vec{\rho}_\mu$ with the third generation of quarks $\psi = (t, b)$

$$\begin{aligned} L^f_\rho &= b_1 \bar{\psi}_L \xi^\dagger i\gamma^\mu [\partial_\mu - ig''\vec{\rho}_\mu \vec{\tau} + ig'/6B_\mu]\xi\psi_L \\ &\quad + b_2 \bar{\psi}_R P \xi i\gamma^\mu [\partial_\mu - ig''\vec{\rho}_\mu \vec{\tau} + ig'/6B_\mu]\xi^\dagger P\psi_R - (\bar{\psi}_L U^\dagger M \psi_R + h.c.) \\ &\quad - \lambda_1 \bar{\psi}_L i\gamma^\mu (\xi^\dagger \mathcal{A}_\mu \xi)\psi_L + \lambda_2 \bar{\psi}_R P i\gamma^\mu (\xi \mathcal{A}_\mu \xi^\dagger) P\psi_R \,. \end{aligned} \tag{1}$$

In the above equation, g'', $b_{1,2}$, $\lambda_{1,2}$ are free parameters, $\vec{\tau} = \vec{\sigma}/2$, where $\vec{\sigma}$ are the Pauli matrices, M=diag(m_t, m_b) and P =diag(1,0). The Goldstone bosons triplet $\vec{\pi}$ enters L^f_ρ through $\xi = \exp(i\pi_k\tau_k/v)$, $U = \xi\xi$ and $\mathcal{A}_\mu = \xi^\dagger(D_\mu U)\xi^\dagger/2$. The relevant parts of the effective chiral Lagrangian can be cast into a very simple form

$$L = ig_\pi M_\rho/v(\pi^-\partial^\mu\pi^+ - \pi^+\partial^\mu\pi^-)\rho^0_\mu + g_V \bar{t}\gamma^\mu t\rho^0_\mu + g_A \bar{t}\gamma^\mu\gamma^5 t\rho^0_\mu \,, \tag{2}$$

where $g_\pi = M_\rho/(2vg'')$, $g_V = g''b_2/(4(1+b_2)) + \mathcal{O}((g/g'')^2)$ are coupling constants of $\rho W_L W_L$ and $\rho t\bar{t}$ interactions. Partial wave unitarity limits for $M_\rho = 700$ GeV are $g_\pi \leq 1.75$ (derived from $\pi^+\pi^- \to \pi^+\pi^-$) and $g_V \leq 1.7$ (derived from $t\bar{t} \to t\bar{t}$).

There are six new parameters – g'', b_1, b_2, λ_1, λ_2 and the ρ mass, M_ρ. We do not have any experimental constraints on M_ρ – the theoretical expectation is around 1–3 TeV since the above stated unitarity constraints are preserved in our model in the processes $W_L W_L \to W_L W_L$, $W_L W_L \to t\bar{t}$ and $t\bar{t} \to t\bar{t}$ for collision energies up to 3 TeV. We do have, however, constraints on g'', b_1, b_2 and λ_1, λ_2. These are due to the corrections that g'', b_1, b_2, λ_1, λ_2 induce in the SM couplings of the Z and W to fermions at low energies (∼90 GeV). The constraints are

$$g'' \gtrsim 10, |b_1 - \lambda_1| \lesssim 0.01, \quad -0.03 \lesssim b_2 - \lambda_2 \lesssim 0.04. \tag{3}$$

Below we assume for simplicity $b_1 = \lambda_1 = 0$. The other reason for this is that, as we can see, the low energy limit on b_1 and λ_1 is more stringent than the low energy limit on b_2 and λ_2. In addition, our results are almost independent of λ_2. Thus we are left only with M_ρ, g'' and b_2 as free parameters.

3. SIGNAL AND BACKGROUND ANALYSIS

3.1. $e^+e^- \to \nu_e\bar{\nu}_e t\bar{t}$

In our calculations of the cross-sections we used two programs – CompHEP [5] and Pythia [6]. As an example we give the total cross-section for the signal process with parameters $M_\rho = 700$ GeV, $\Gamma_\rho = 12.5$ GeV, b_2=0.08, g''=20, calculated with no cuts with CompHEP. For three different energies of collision, $\sqrt{s} = 0.8, 1.0, 1.5$ GeV, we get $\sigma(e^+e^- \to \nu_e\bar{\nu}_e t\bar{t}) = 0.66, 1.16, 3.33$ fb, respectively. In order to have an independent check we performed calculation for the same parameters and the same collision energies using also Pythia. The cross-sections obtained were 0.31, 0.81 and 3 fb, respectively. Hence, as expected, the agreement between CompHEP and Pythia becomes better with increasing collision energy since Pythia uses an effective vector boson approximation and a subset of fusion diagrams that become dominant with increasing $\sqrt{s}$.

In Fig. 2 are plotted the differential cross-sections of $e^+e^- \to \nu_e\bar{\nu}_e t\bar{t}$ for the collision energy 1 TeV and for three models – no-resonance, ρ-resonance with the above set of parameters, and SM Higgs with $M_H = 700$ GeV. As the picture shows the distribution for Higgs is rather broad while in the one for ρ one can see a narrow peak centered at $m_{t\bar{t}} = 700$ GeV rising above the continuum background.

With Phytia we also calculated the cross-sections of two major background processes: $e^+e^- \to t\bar{t}\gamma$ and $e^+e^- \to e^+e^-t\bar{t}$ that represent the reducible background. The irreducible background is represented by the "No resonance" model, that is a model, in which we set M_ρ equal to a very large value. In this way the ρ-resonance is effectively removed from the particle spectrum, *i.e.* the calculation includes only processes in which ρ doesn't appear and we performed it with CompHEP.

In order to reduce the background we imposed the following sets of cuts: For the collision energy $\sqrt{s} = 0.8$ TeV we set:

$$\begin{aligned}
&500 < m_{t\bar{t}} < 750 \text{ GeV}, \quad -0.8 < \cos\theta_{t\bar{t}} < 0.8, \\
&0 < E_t, E_{\bar{t}} < 380 \text{ GeV}, \quad 15 < p_T(t\bar{t}) < 300 \text{ GeV}, \\
&20 < p_T(t), p_T(\bar{t}) < 330 \text{ GeV}, \quad 50 < M_{rec} < 800 \text{ GeV}, \\
&90 \text{ GeV} < E_{miss}, \quad -0.96 < \cos\theta_{pmiss} < 0.96.
\end{aligned} \tag{4}$$

The total background was reduced from 301.6 fb to 0.13 fb and the signal decreased from 0.66 fb down to 0.2 fb. For the collision energy $\sqrt{s} = 1$ TeV we set:

$$500 < m_{t\bar{t}} < 900 \text{ GeV}, \quad -0.8 < \cos\theta_{t\bar{t}} < 0.8, \tag{5}$$

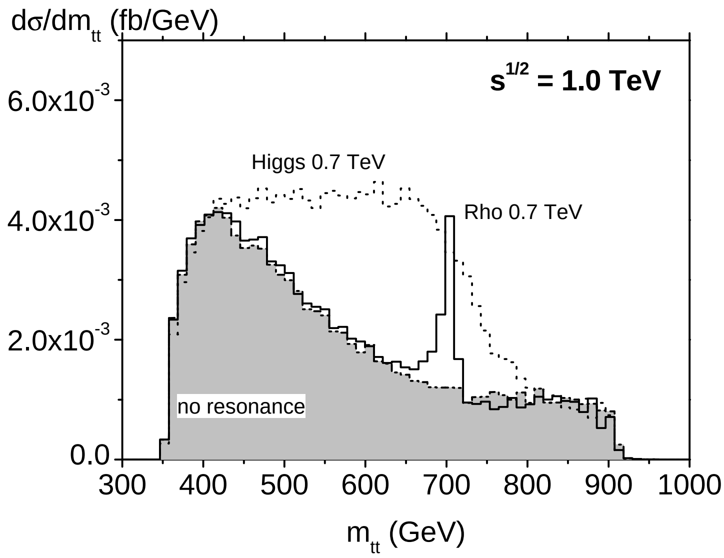

Figure 2: Differential cross-sections of $e^+e^- \to \nu_e\bar{\nu}_e t\bar{t}$ as a function of $m_{t\bar{t}}$ – comparison of ρ (M_ρ=700 GeV, Γ_ρ = 12.5 GeV, b_2=0.08, g''=20) with the SM Higgs boson (M_H = 700 GeV) and no-resonance.

$$0 < E_t, E_{\bar{t}} < 480 \text{ GeV}, \quad 15 < p_T(t\bar{t}) < 400 \text{ GeV},$$
$$20 < p_T(t), p_T(\bar{t}) < 400 \text{ GeV}, \quad 150 < M_{rec} < 1000 \text{ GeV},$$
$$100 \text{ GeV} < E_{miss}, \quad -0.96 < \cos\theta_{pmiss} < 0.96.$$

The total background was reduced from 207.3 fb to 0.035 fb while the signal dropped from 1.16 fb down to 0.16 fb.

The impact of some of the cuts in (5) on signal and background for $e^+e^- \to \nu_e\bar{\nu}_e t\bar{t}$ at $\sqrt{s}$ = 1 TeV and luminosity $\mathcal{L}$=500 fb^{-1} is depicted in Fig. 3. As the picture demonstrates, the reduction of both the signal and the background is after cuts markedly large. However, the ratio signal/background increases considerably as well.

The statistical sensitivity of the process to distinguish between the model with the vector resonance and "no-resonance" model (backgrounds included) is given by the following relation

$$R = \frac{|N(\rho) - N(\text{no-resonance})|}{\sqrt{N(t\bar{t}\gamma + e^+e^-t\bar{t}) + N(\text{no-resonance})}}, \tag{6}$$

where N denotes the number of events. The same background is assumed for both resonance and no-resonance models. In Fig. 4 we show R contours

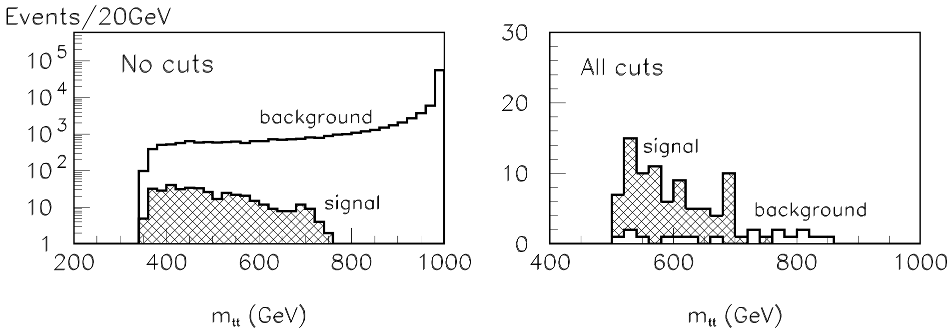

Figure 3: The results of applying cuts (5), except the third and the fifth cut, to $e^+e^- \to \nu_e\bar{\nu}_e t\bar{t}$. The number of events per a 20 GeV bin as a function of $m_{t\bar{t}}$ is plotted for the ρ-channel with the parameters of the ρ-resonance M_ρ=700 GeV, Γ_ρ = 12.5 GeV, b_2=0.08, g''=20. The collision energy is $\sqrt{s} = 1$ TeV and the integrated luminosity is 500 fb^{-1}.

in the g'' - b_2 parametric space at the energy of 0.8 and 1 TeV and the integrated luminosity of 200 fb^{-1}.

3.2. $e^+e^- \to t\bar{t}$

This process shows surprisingly good sensitivity to the presence of the ρ-resonance. While we expect ρ to couple strongly to the top quark and not to the electron, it turns out that the latter coupling (induced through ρ mixing with photon and Z-boson) is large enough to generate clear peak rising above continuum background.

In Fig. 5 we show the total cross-sections as a function of the CMS energy in the region around the peaks of the vector resonances with a) $M_\rho = 0.7$ TeV and b) $M_\rho = 1.5$ TeV both with and without the effects of initial state radiation (ISR) and beamstrahlung (BS). In Fig. 5a two resonances are depicted – broader with parameters $b_2 = 0.08$, $g'' = 20$, $\Gamma = 12.5$ GeV and narrow with parameters $b_2 = 0.003$, $g'' = 20$, $\Gamma = 0.25$ GeV. The irreducible (continuum) background and the line that corresponds to the statistical significance $R = 5$ are shown as well.

4. CONCLUSIONS

We have studied a new vector resonance from SESB in $e^+e^- \to \nu\bar{\nu}t\bar{t}$ and $e^+e^- \to t\bar{t}$ at future e^+e^- colliders operating at 1 TeV energy scale.

The first process contains $W_LW_L \to \rho \to t\bar{t}$ scattering as its subprocess and is potentially sensitive to the $\rho-t\bar{t}$ coupling g_V. The size of this coupling

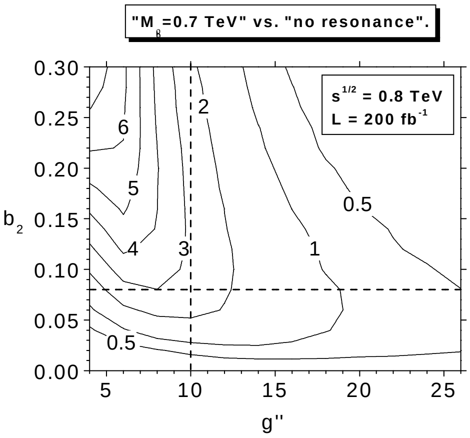

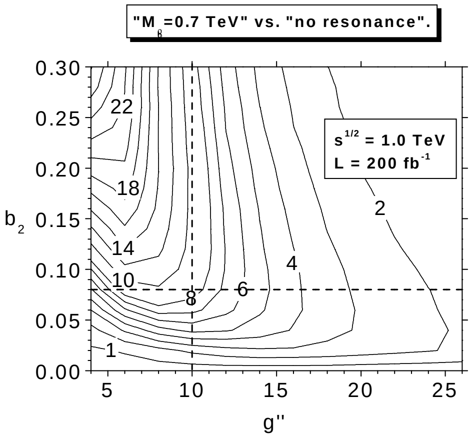

Figure 4: Sensitivity contours (see Eq. (6)) in the g'' - b_2 parametric space at the energy of 0.8 and 1 TeV and the integrated luminosity of 200 fb^{-1}. The mass of the ρ-resonance is 0.7 TeV. The cuts (4) and (5) were used, respectively, except that the first cut in both cases was changed to $670 < m_{t\bar{t}} < 730$ GeV. The values of R are shown on the contours. The dashed lines are low-energy limits. The allowed regions are in the lower right corner.

could hint on the mechanism of the top mass generation. We found (working at the level of undecayed top quarks) that statistical significance R is as large as 8 for M_ρ =700 GeV for certain regions of the parameter space allowed by the low energy constraints at 1 TeV collider.

The second process, $e^+e^- \to t\bar{t}$, is sensitive to the vedctor resonance only if its coupling to the electron is not negligible. This is exactly the case of our model. In fact, it is the most promising process in this case. It requires that the collider be able to scan the whole energy scale up to the maximum energy to find the resonance peak. Our results show that it should be possible to discover ρ resonances with $b_2 = 0.08$ if the scanning luminosity is 1 fb^{-1}.

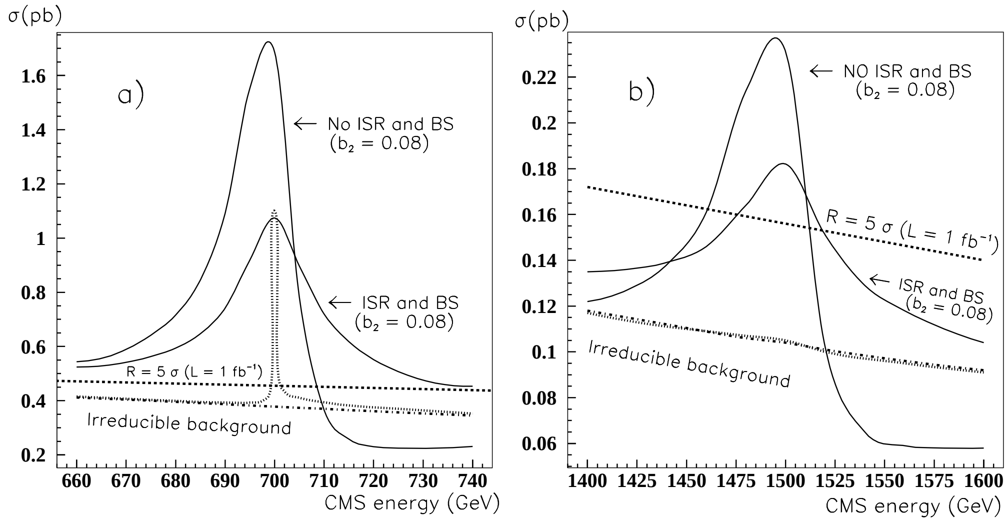

Figure 5: **a)** $M_\rho = 700$ GeV. The solid curves represent the total cross-sections as a function of CMS energy without/with initial state radiation (ISR) and beamstrahlung (BS) corrections for a resonance with $b_2 = 0.08,\ g'' = 20,\ \Gamma = 12.5$ GeV. The dotted line (narrow peak) corresponds to a resonance with $b_2 = 0.003,\ g'' = 20,\ \Gamma = 0.25$ GeV(ISR & BS included). The dash-dotted straight line represents irreducible (continuum) background with ISR & BS. The dashed line shows the boundary at which the statistical significance $(S/\sqrt{B})$ equals 5 assuming the scanning luminosity $L_{scan} = 1$ fb^{-1}. **b)** Same as a), except that $M_\rho = 1500$ GeV and the width of the two resonances is changed accordingly to 40.9 GeV and 9.7 GeV. The latter resonance cross-section is almost identical with the irreducible background.

[1] T. L. Barklow et al.: *Strong Coupling Electroweak Symmetry Breaking*, Working Group Summary Report from the 1996 DPF/DPB Summer Study New Directions for High Energy Physics, Snowmass, Colorado, June 25 – July 12, 1996, [hep-ph/9704217], and references therein.

[2] E. R. Morales, M. E. Peskin: *Proceedings of the International Workshop on Linear Colliders*, Sitges, Barcelona, Spain, April 28 – May 5, 1999, [hep-ph/9909383].

[3] M. Gintner, I. Melo, *Acta Phys. Slov.* **51**, 139 (2001)

[4] R. Casalbuoni et al., *Phys.Lett.* **B155**, 95 (1985); D. Dominici, *Riv.Nuovo Cim.***20**, 1 (1997); R. Casalbuoni et al., *Phys.Lett.* **B258**, 161 (1991)

[5] E. Boos et al. [CompHEP Collaboration], *Nucl. Instrum. Meth.* **A534**, 250 (2004) [hep-ph/0403113]; CompHEP - a package for evaluation of Feynman diagrams and integration over multi-particle phase space. User's manual for version 3.3, hep-ph/9908288

[6] T. Sjöstrand, *Computer Physics Commun.* **82**, 74 (1994)